Available online at www.sciencedirect.com

ScienceDirect

Procedia Engineering 213 (2018) 437–447

Procedia Engineering

www.elsevier.com/locate/procedia

7th International Conference on Fatigue Design, Fatigue Design 2017, 29-30 November 2017, Senlis, France

A comparative study of various joining techniques fatigue behaviour focusing on stiffness degradation

Peter Rösch[a,*], Thomas Bruder[a], Thilo Bein[b]

[a]*BMW Group, Knorrstr. 147, 80788 Munich, Germany*
[b]*Fraunhofer Institute for Structural Durability and System Reliability LBF, Bartningstr. 47, 64289 Darmstadt, Germany*

Abstract

The design of parts and structures in the vehicle development process is highly influenced by strength and stiffness requirements. Under cyclic loading a change in the local stiffness of joints can be observed which motivates analyses in order to tackle stiffness changes in structures. The fatigue and stiffness behaviour has been obtained for several joining techniques and material combinations: spot and seam welds, remote laser welds and high velocity bolting for steel and/or aluminium partner sheets. Specimens under shear and peel loading as well as hat profiles under torsion have been tested under constant amplitude loading. Quasi-static tests and micrographic evaluations have been conducted in order to determine material parameters and the setup of FE models. Online stiffness measurements during fatigue life have been performed. In this paper an approach to describe degradation in specimens representing a joint detail is presented. The stiffness degradation curves for the various joining techniques are compared and a numerical description of the stiffness degradation behaviour for further simulations is derived. The concept of simulating stiffness changes in conventional joining techniques is introduced. First numerical analyses of stiffness changes in spot welded specimens are presented. Several sensitivity analyses, e.g. with regard to R-ratio or loading amplitude, are performed in order to check the numerical stability of the implemented method.

Peer-review under responsibility of the scientific committee of the 7th International Conference on Fatigue Design.

Keywords: Stiffness degradation; automotive joining techniques; numerical approach; fatigue life simulation

1. Introduction and Motivation

Strength and stiffness requirements highly influence the dimensions and therefore also the weight of components and structures. In order to meet increasing customer demands and to reduce the overall vehicle emissions, light weight construction is an essential aspect in the vehicle development process. To achieve a lightweight construction a diversity of materials and joining techniques is applied. To illustrate the usage of connections in the automotive industry, Figure 1 shows the spot and seam welds in the current BMW 7 series. More than 5000 spot welds are used in the vehicle chassis. Especially joints are known to change their stiffness during fatigue life which can have an impact on the local stress state. As a result of local stiffness changes, fatigue life may be affected positively or negatively. An elongation of fatigue life can occur if, due to changes in the local stiffness, stresses redistribute in areas which have

*Corresponding author: Tel.: +49-89-382-36438
Email address: peter.roesch@bmw.de (Peter Rösch)

1877-7058
Peer-review under responsibility of the scientific committee of the 7th International Conference on Fatigue Design.
10.1016/j.proeng.2018.02.043

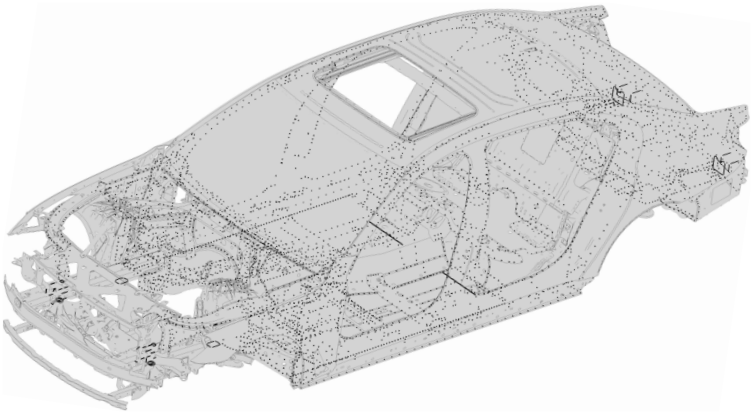

Fig. 1. Spot weld connections in the current BMW 7series

observed lower stresses in the previous fatigue life. Under different conditions a reduction of fatigue life may also be a consequence of degradation. The stiffness behaviour often depends on loading direction and load level, material combination or the used joining technique, respectively. In the first part of the paper a general comparison of the fatigue and stiffness behaviour of various joining techniques, material combinations and loading conditions is performed.

For a consequent light weight construction, novel methodologies are needed to predict the materials fatigue behaviour as stiffness changes are not taken into account in currently used fatigue analyses tools yet. Therefore increased safety factors are used in the design process which lead to an unnecessary increase in the overall vehicle weight. In the second part of this paper a model tackling the issue of stiffness degradation is introduced in order to design for fatigue and stiffness behaviour of spot welded specimens under constant amplitude loading. The established methodology will be derived using shear and peal specimens and later applied to component-like structures (e.g. the hat specimen).

2. Theoretical Background

2.1. Joining process of the introduced techniques

In total four different joining techniques are assessed and introduced briefly in this paper. The techniques include resistance spot welding (RP), arc welding (SW), remote laser welding (RLS, also referred to as scanner welding) and high velocity bolting (HVB, also referred by the brand name RIVTAC ® [1] or nailing [2]). Figure 2 shows a schematic representation of the joining processes.

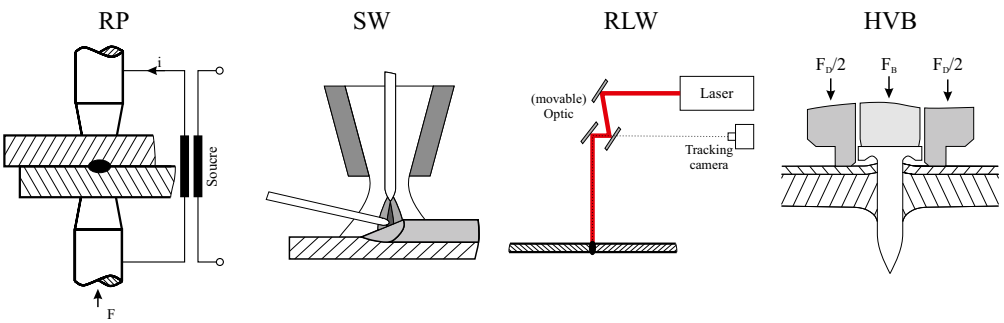

Fig. 2. Schematic representation of selected joining processes [1, 3, 4]

The RP and SW joining process are commonly known and therefore will not be described here in detail. A main advantage of remote laser welding is the manufacturing speed and that only a single-side accessibility to the specimen is necessary. The laser can be guided using a movable optic and can be positioned in distance of the joined components [4]. HVB is a force- and / or form-closed joint [1]. During the HVB joining process a nail-like auxiliary joining part

is driven into the not pre-punched joining partners under high velocity. The process consists of four steps. In the first step the nail is positioned on the joining partners. In the second step it enters the material followed by the penetration of the joining partners (third step). The fourth step braces the joint [1].

2.2. Various fatigue assessment approaches

The fatigue assessment of joints can be described using conventional fatigue life models, phenomenological models for residual stiffness and strength or progressive damage models. Fatigue life models use SN curves and propose a failure criterion based on a classical damage accumulation hypothesis, e.g. Miners law. Damage mechanisms are not taken into account in detail and excessive experimental testing is necessary [10]. Conventional fatigue life models are often used to assess the fatigue life of the introduced joining techniques. As a numerical approach to simulate the stiffness behaviour of spot-welded specimens is shown in the following sections, relevant fatigue assessment approaches are introduced briefly.

For the fatigue life assessment of spot welded components the FESPOW concept is often used in the automotive industry [5]. The spot weld nuggets are represented with beam elements and six general forces are determined acting on the nugget. Beam cross-section forces and moments are used to derive the stress state in the base material which will be evaluated during fatigue life. With this approach only a single SN curve, derived from a variety of cyclic tests on single spot weld specimens, is necessary compared to an approach in which the stress in the neighbouring elements of the nugget is evaluated (FEMFAT Spot) [6]. Using the FEMFAT Spot approach different SN curves are applied for damage accumulation, depending on the local stress tensor (tension/compression, shear or a combination of both). The SN curves are derived using component-like specimens, e.g. H or KS specimens [7]. In addition to the introduced assessment approaches for spot welds notch-stress or strain approaches are available but rarely used in the automotive industry. FE models used for the introduced approaches are shown in Figure 3. Phenomenological and

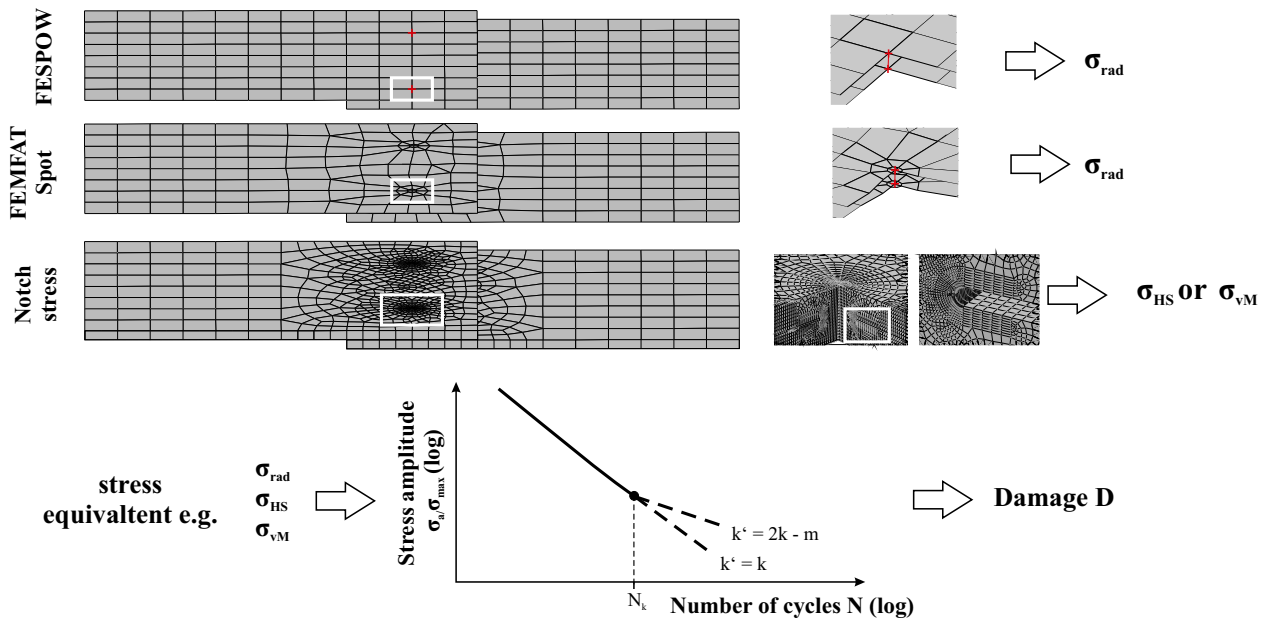

Fig. 3. FESPOW, FEMFAT Spot and notch-stresss fatigue assesment approach, based on [5]

progressive damage models are widely applied in the fatigue assessment of carbon fibre reinforced plastics (CFRP) [8], but rarely used for the assessment of joints or base materials. Phenomenological models describe the changes in the specimen stiffness and strength with regard to macroscopic observable properties [9]. In residual stiffness models failure occurs when the specimen stiffness undercuts a defined level. In the literature several failure levels can be found, e.g. when when the secant modulus in fatigue decreases to within the range of the secant modulus of static failure [10]. Progressive damage models describe the changes of specimens as a function of one or more selected damage variables [9].

In the following sections a residual stiffness model, based on conventional fatigue life calculations, is introduced. It is used not only to assess the fatigue life but also to describe the stiffness behaviour during its fatigue life.

2.3. Experimental fatigue life and crack propagation of spot welded specimens and structures

In the last 35 years fatigue life of spot welded specimens and structures has been investigated thoroughly. The complexity in its assessment results from various challenges compared to non welded structures, for example the [11]:

- determination of different material properties and hardnesses within the spot weld (base material, nugget or heat affected zone),
- uncertain residual stresses in the spot weld due to the manufacturing process,
- uncertain micro-geometry on the spot weld's notch,
- unknown crack initiation and propagation areas.

Especially the topic mentioned in the last bullet point is highly dependent on the local stress state and the load level of the tested specimens and structures, as indicated in Figure 4 which shows different crack initiation and propagation areas experimentally and numerically obtained by several researchers [11]. Figure 4 a) shows a crack initiation and propagation behaviour which often can be observed in the high cycle fatigue regime under tensile shear loading, according to Draisma and Overbeeke [12, 13]. Two types of fracture can be observed - plate and joint face fracture. In the case of plate fracture, which occurs mainly in combination with larger spot diameters d_{spot}, small cracks initiate transverse to the local structural stress. Under joint face fracture, which often occurs in combination wiht smaller spot diameters, shear cracks start at the flank sides of the spot weld [13]. As shown in Figure 4 b) Satoh et al determined the effect on fatigue crack propagation due to a heat-affected zone (HZ) under high- and low-cycle fatige [13, 14]. Under low-cycle fatigue the crack starts from the unaffected base material. During high-cycle fatigue the crack often starts at the weld notch. Yuuki et al. computed crack propagation directions according to a maximum tangential stress criterion and compared them to actual crack paths experimantally obtained, as displayed in Figure 4 c) [13, 15]. The specimens were tested under tensile-shear (TS), cross-tension (CT) and angle-to-plate (AP) loading with different load levels ΔF, classified in small, medium and large load levels.

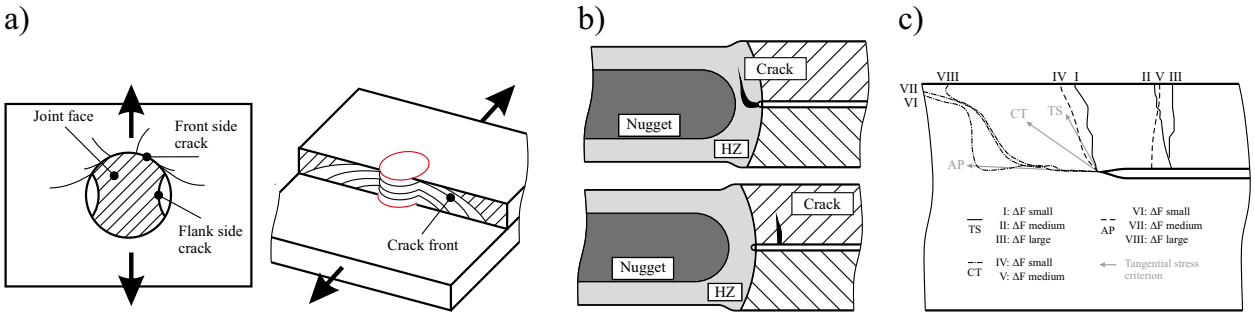

Fig. 4. Crack initiation and propagation areas for different loading conditions and heat affected zones (HZ) after a) Draisma et al. [12], b) Satoh et al. [14], c)Yuuki et al. [15] , summarized in [11]

3. Experimental Results

3.1. Assesed Materials, specimens and joining techniques

A summary of the assessed joining techniques, material combinations and specimen geometries can be found in Table 1. In addition to the results obtained at Fraunhofer LBF and Montanuniversitt Leoben results of the research project FAT142 [16] and FAT239 [5] are shown. Several specimens have been used to obtain the experimental results, as shown in Figure 5. As a representation of the joint a spot weld is shown. Shear (SEZ), peal specimens (SAZ) and the KS specime are tested in order to get an experimental database of the fatigue behaviour of the joint itself. The hat specimen represents a more component-like specimen with overall ten RP, RLS, HVB / 1 SW joints on each side. The fatigue tests with the KS specimen have been conducted using different load directions (0°, 15°, 30°, 60° and 90°),

Table 1. Tested material, thickness and specimen geometry

Specimen	Material	l_1	l_2	l_3	l_4	l_5	l_6	b	t
						in mm			
RP-SEZ1	CR380	305	160	35	17.5	17.5	35	70	1.5
RP-SEZ2	H320LA+ZE								1.75
RP-SEZ3	DX54D+ZE100	375	230	50	25	25	50	100	1.8
RP-SEZ4	H320LA & DX54D								1.75 & 1.8
RP-SAZ1	CR380	260	160	35	20	17.5	35	70	1.5
RP-SAZ2	H320LA+ZE								1.75
RP-SAZ3	DX54D+ZE100	380	280	50	25	25	50	100	1.8
RP-SAZ4	H320LA & DX54D								1.75 & 1.8
RP-HP	CR380	500	350	15	30	50	50	80	1.5
SW-SEZ	AL5-STD	200	100	20	-	-	-	48	2
SW-SAZ	AL5-STD	140	70	35	20	-	-	48	2
SW-HP	AL5-STD	500	350	6.5	30	50	-	80	2
RLS-SAZ	AL5-STD	110	60	10	50	100	-	48	1.5
RLS-HP	AL5-STD	500	350	3	30	50	-	80	1.5
HVB-HP	CR380 & AL5-STD	500	350	6.5	30	50	-	80	1 & 4

materials (Mat1 = DC04, Mat2 = DP-K 30/50), sheet thicknesses (t_1 = 0.8 mm, t_2 = 1.5 mm and nugget diameters (d_{N1} = 4.4 mm, d_{N2} = 6 mm). Further informations about the testing procedure and details on the KS specimen geometry can be found in [17]. The hat specimen has been tested with a alternating load ($R = -1$). The remaining

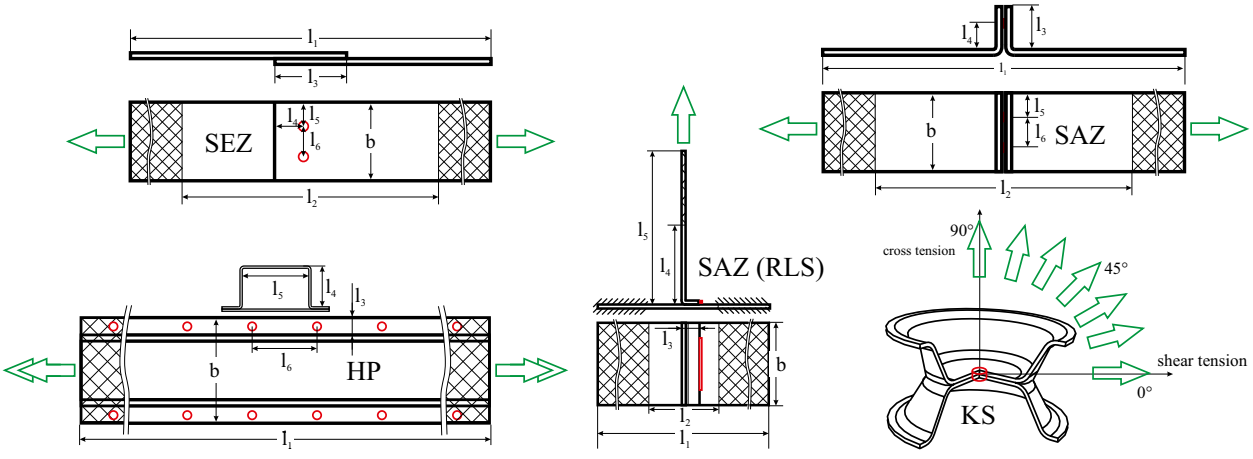

Fig. 5. Geometry of shear, peal, hat and KS specimen [17]

specimens have been tested under tension loading (R = 0.1).

3.2. Micrographic analysis and experimental fatigue life results

For each joining technique micrographic analysis is performed in order to determine the local geometry. The obtained geometry is used for detailed FE modelling. In Figure 6 the results are shown, the detailed (average) spot weld geometry is displayed in Table 2. The average values are computed using n=4 samples. Especially during the RLS seam weld manufacturing process big parts of the upper metal sheet's front edge did melt. A hardness measurement through several points of the RLS weld did show an quite constant hardness through the weld. The HVB micrographic analysis shows small gaps between the joining partners and also between the nails head and the upper sheet. It cannot be fully

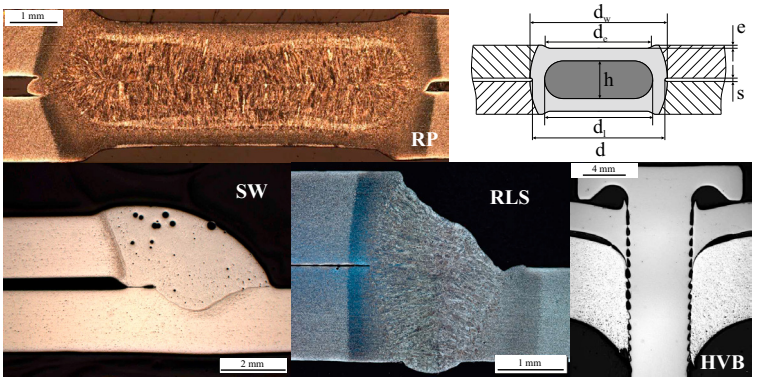

Fig. 6. Micrographic shot of the shear (RP, SW), peal (RLS) and hat specimens (HVB)

Average value in mm	
d_l	7.69
d	8.22
d_w	8.68
d_e	6.88
e	0.26
h	2.2
s	0.32
t	1.5

Table 2. Spot weld geometry according to [18]

ruled out, that these gaps result from the grinding and polishing during the analysing process.

Selected SN curves of the tested specimens are shown in Figure 7. The nominal stress amplitudes are normalized using the maximum obtained nominal stress amplitude under constant amplitude loading. The shear and peal specimens (Figure 7 a)) show an inverse slope k between $k = 2.53$ (RP SAZ1) and $k = 5.34$ (SW SEZ). The specimen geometry

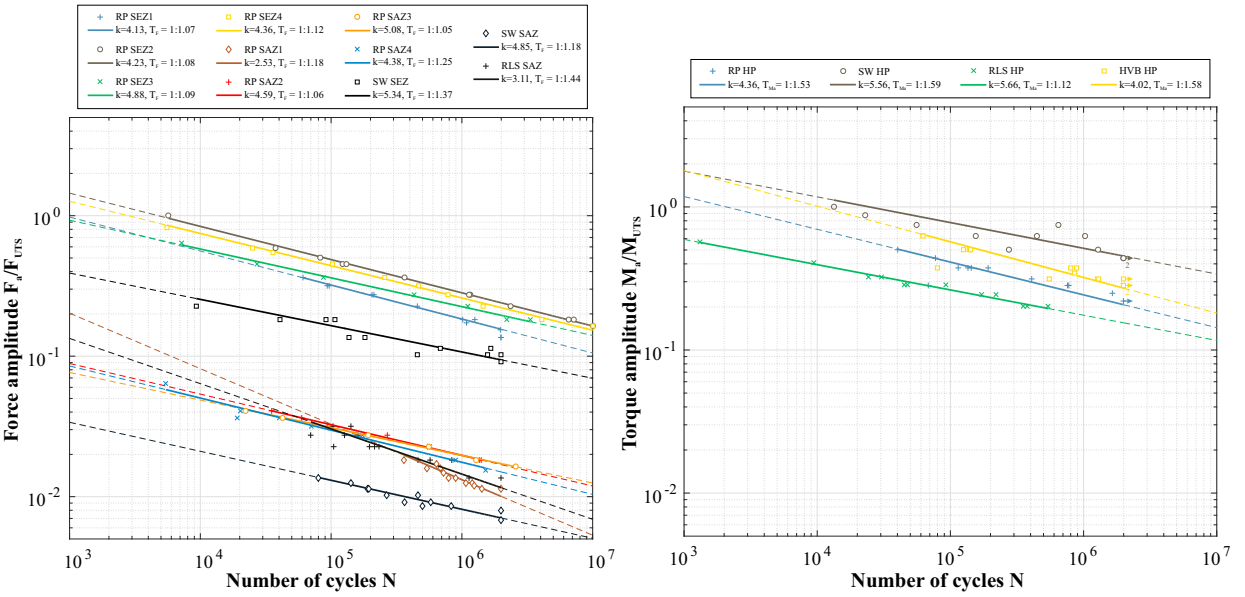

(a) RP, SW, RLS - shear and peel specimen, $R = 0.1$

(b) RP, SW, RLS, HVB - hat specimen $R = -1$

Fig. 7. SN curves of the presented specimens / joining techniques

divides the SN curves in two groups. The SW SEZ specimen is located between the two groups. As it would be expected overall fatigue life of the SEZ specimens is higher compared to the SAZ specimens. A maximum scatter of the SN curves $T_F \leq 1 : 1.59$ (10 % / 90 %) is observed.

The HP specimen's scatter (see Figure 7 b)) is slightly higher except the RLS HP. There are two failure modes present for the RLS specimen. At low load levels cracks initiate in the base material at the beginning or end of a seam weld and propagate in 90° direction to the edge through the steel flange. At high load levels the weld breaks in the joining plane. A crack propagation is not observed.

3.3. Stiffness degradation during fatigue life

A comparison of the stiffness behaviour of the introduced joining techniques can be found in Figure 8. The stiffness behaviour during cyclic testing is observed using the displacement data of the test rigs actuator and (if possible) also the local displacement data measured with an extensometer. Subfigure a) shows the SEZ and SAZ specimens whereas subfigure b) shows the HP's stiffness behaviour. The stiffness of the RP SAZ specimen decrease right from the start of the experiment. The steps in the RLS HP specimens stiffness may result through cracks in the seperate welds. This could be verified assessing DMS measurements in next to one RLS weld but needs further investigation. The HVB specimen shows an increase in stiffness until approximately 10 % of fatigue life is reached. This can be observed independently from the applied load level through all tests. This could result from setting or relative movement of the bolt but also need further investigations.

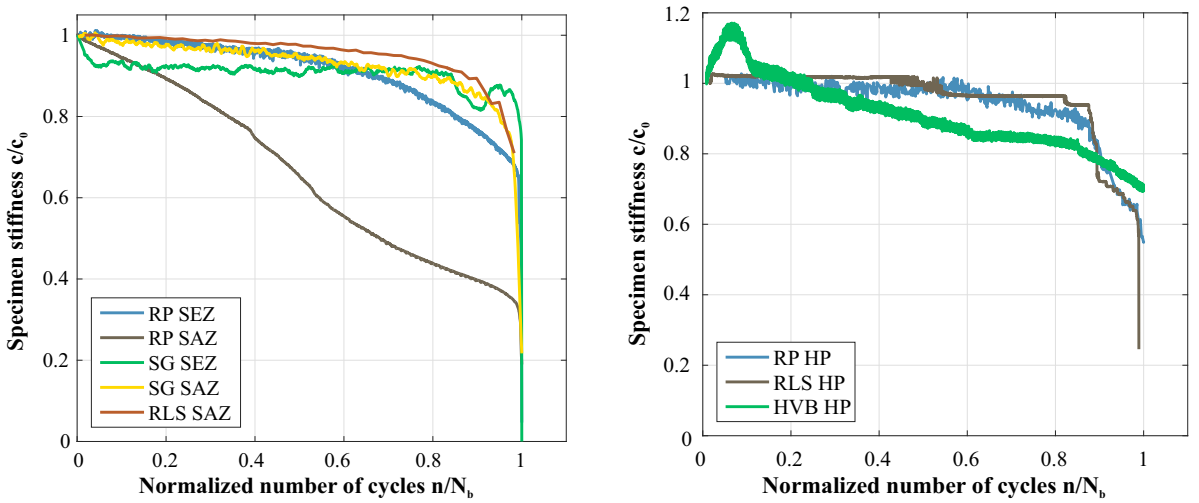

(a) Stiffness behaviour SEZ, SAZ specimen

(b) Stiffness behaviour HP specimen

Fig. 8. Stiffness degradation of selected KS specimen with different loading directions, materials and weld geometry

In order to setup a numerical approach describing stiffness changes several assumptions need to be made and verified using experimental data. The approach presented in the following section is based on two main assumptions:

1. The stiffness behaviour of a certain stress state can be approximated using the linear combination of the stiffness behaviour of two extreme stress states (e.g. shear or cross tension).
2. The normalized stiffness behaviour is (almost) independent from the welding parameters, metal combinations or sheet thickness.

A first indication about the permissibility of the first assumption is shown in Figure 9 a), which shows the stiffness behaviour of the KS specimens under different loading directions. Excluding the 0° direction the 15° and 90° degree direction represent the lower and upper limit of the stiffness behaviour. The 0° stiffness behaves somehow different. One explanation is the load level of 1500 N for which the data was obtained. As it is the highest load level of the SN curve crack initiation can occur at different locations (as shown in the theoretical background). This may result in a non-comparable stiffness behaviour. Indications for the permissibility of the second assumptions are shown in Figure 9 b). Different materials, nugget diameters and sheet thickness are compared at medium load levels with 30° load direction. Almost no sensitivity to the changed parameters can be observed. Only the stiffness result of the second material tested under a low load level shows deviations to the average behaviour. As it does not match with the test on a slightly higher load level with the same parameter combination, it will be considered as an exception and not taken into account for further analyses.

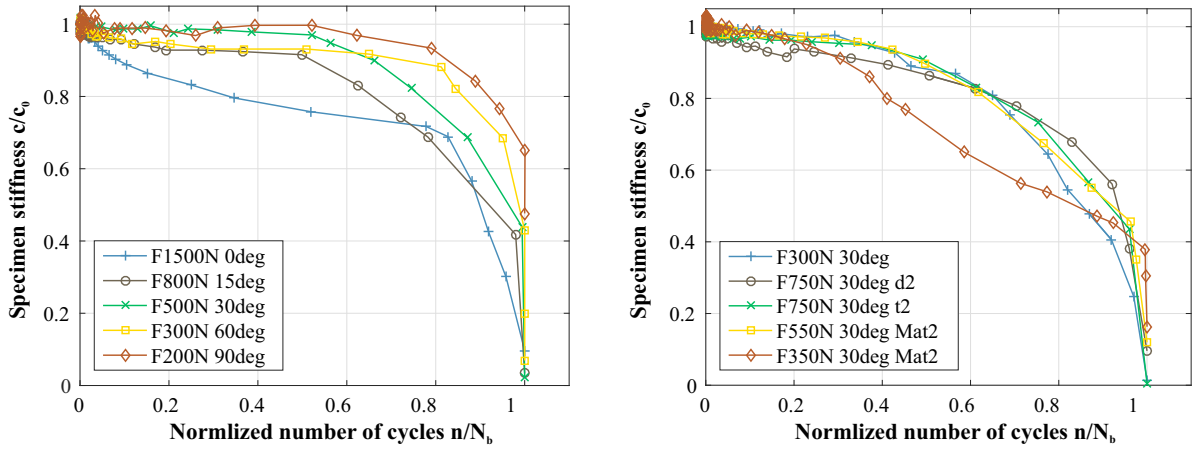

(a) Alternation of loading direction 0°-90°

(b) Alternation of Material, thickness & nugget diameter @ 30° loading

Fig. 9. Stiffness degradation of selected KS specimen with different loading directions, materials and weld geometry

4. Numerical Analyses

4.1. Numerical approach DegraRP

To simulate stiffness degradation an iterative computation process is used. Figure 10 introduces the basic idea of the DegraRP methodology. A conventional fatigue life simulation (represented with the black outline in Figure 10) is based on the quasi-static FE results, SN curves and damage accumulation using Miners law and allowable damage sum D. Changes in the local stiffness are not considered at all. To be able to consider the stiffness behaviour during fatigue life simulation, the stiffness of the FE model needs to be adapted after certain thresholds have been reached (represented with the additional components with a green outline in Figure 10). A partial damage accumulation computation is conducted after which an evaluation of the current stiffness degradation state is performed. This evaluation is based on a stiffness degradation curve, describing stiffness as a function of the accumulated damage D derived from experimental data. Two additional parameter sets are necessary to determine boundaries for a recomputation with an adapted FE model. The parameter sets can be divided into material and computation (status) parameters. In a first step

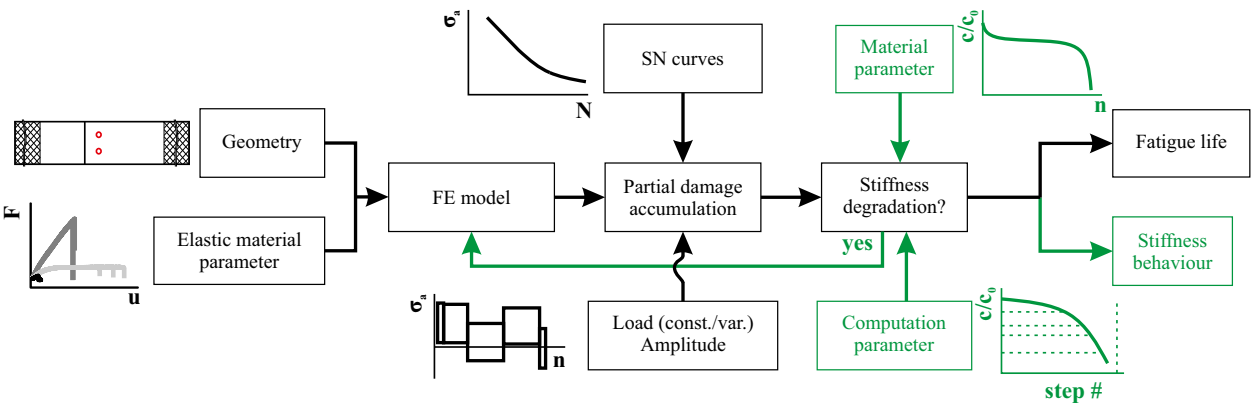

Fig. 10. Nuemrical stiffness degradation approach DegraRP

the stiffness degradation curve is assumed to be a simple power law, see Equation (1). The material parameters c_i are determined using a method of least squares to fit the functions parameters to the experimental data. In this project a power law of $i = 6$ is used. As the main goal is to show that the principal methodology is capable to simulate stiffness

degradation. Deriving a more accurate degradation law will be focus of future research.

$$stiffness(D) = \sum_i c_i \cdot D^i \tag{1}$$

The stiffness degradation law is valid for the loading direction, material combination and weld parameters it has been derived from. As stated in the experimental section, the degradation law of another loading direction can be approximated using a combination of known degradation laws. For example for a 45° direction the degradation law may be approximated using 50 % of a 0° and 50 % of a 90° loading direction degradation law. This results in only little testing effort necessary, if applicable.

The implemented method uses in total five status parameters for the computation, as displayed in Figure 11 a). Additionally to the illustrated status parameters, the parameter *GlobalAllowedRelativeNumber* (GARN) describes the percentage of elements which are allowed to exceed the status parameters and need to be identified for each FE model independently. The status parameters *GlobalUndoStiffnessRelative* (GUS) and *GlobalContinueWithInputStiffnessRelative* (GCS) provide the boundaries for each computation step [19]. The parameter *GlobalFinishStiffnessAbsolute* provides the allowed remaining local stiffness. After the *MaxNumberOfRuns* the computation is stopped regardless of the current state of degradation. As indicated in Figure 11, the computation step from 1 to 4 would be rejected in the implemented software, as it exceeds the boundaries. A step from 1 to 2 or directly to 3 would be accepted. The parameter NZR is used for the maximum number of cycles for each computation step. To be able to change the stiffness of selected spot welds in the FE model a correlation between stiffness and the spot welds FE parameters is necessary. Possible parameter to adapt the FE mesh of the spot weld are the Young's modulus of the spot / beam material, the beam diameter d_B or the FE mesh itself. The adaption of the beam diameter has proven to be suitable as changes in the FE mesh would be to complicated in bigger FE models and changes in the Young's modulus led to numerical unstable results. Figure 11 b) shows the correlation between a target degradation and the beam diameter. In

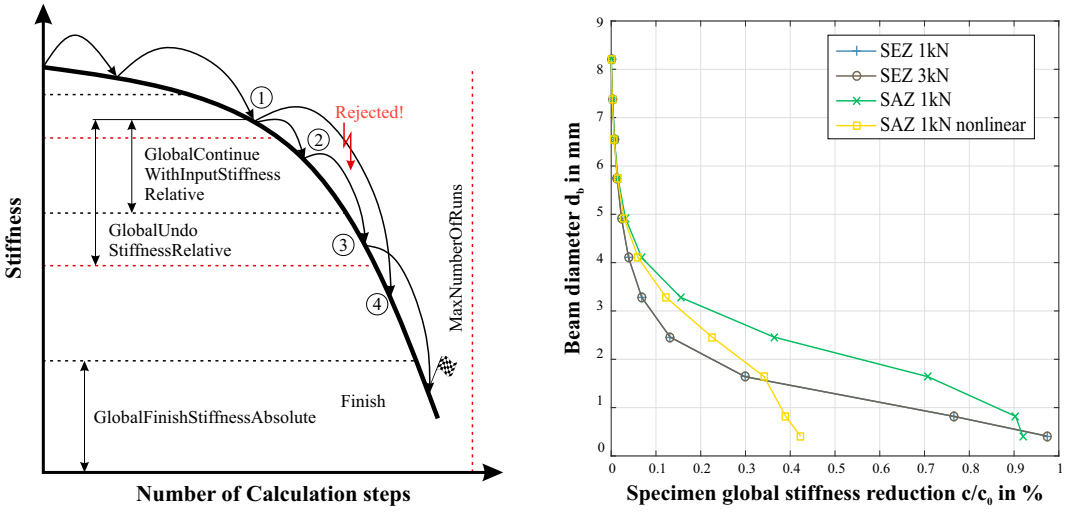

(a) Computation parameters [19]

(b) FEMFAT spot beam diameter as a function of residual stiffness of the spot weld

Fig. 11. SN curves of the presented specimens / joining techniques

order to identify the parameters, several convergence and sensitivity studies are conducted. As a result the parameter set displayed in Table 3 (derived for the shear specimen) will be used in this project.

4.2. First results and solver performance

The introduced DegraRP model is applied to the hat specimen, with material parameters derived from the experimental fatigue results using shear and peel specimens. The results are displayed in Figure 12. In the upper picture the HP specimen's FE model is displayed and four selected hot spots (HP) are highlighted. In the lower figure the numerical

Table 3. Material and status parameter set

Material parameters							Status parameters				
c_0	c_1	c_2	c_3	c_4	c_5	c_6	GCS	GUS	GARN	GFSA	NZR
0.98	0.66	-8.77	40.62	-86.17	83.92	-30.73	0.975	0.8	0.2	0.1	7000

obtained stiffness behaviour is compared to actual test data of the HP specimen with a load of $M_a = 200\,\text{Nm}$. The stiffness behaviour can be described quite accurate until the failure (breakage of the specimen) in the fatigue test. At this point the model cannot predict the failure, computation stops at approx. $N_{num} = 77000$ cycles. Although the basic failure mechanisms of the specimen are represented correctly, the ultimate failure cannot be described yet. At first the spots in the middle of the specimen (HS1 and HS2) show the highest drop in their stiffness. This results in a decrease of the load transferred at these spot welds. After a remarkable decrease in the stiffness at HS3 the specimen finally fails near the clamping at HS4, which is physically quite reasonable but could not be observed during testing as the experiment is stopped at a certain torsion angle. In Table 4.2 selected computation results for the computation steps (#1 – #6) highlighted in Figure 12 are shown. D_{it} represents the damage obtained for each computation interval. The HS with the highest damage in each iteration step is highlighted. The first results of the DegraRP approach

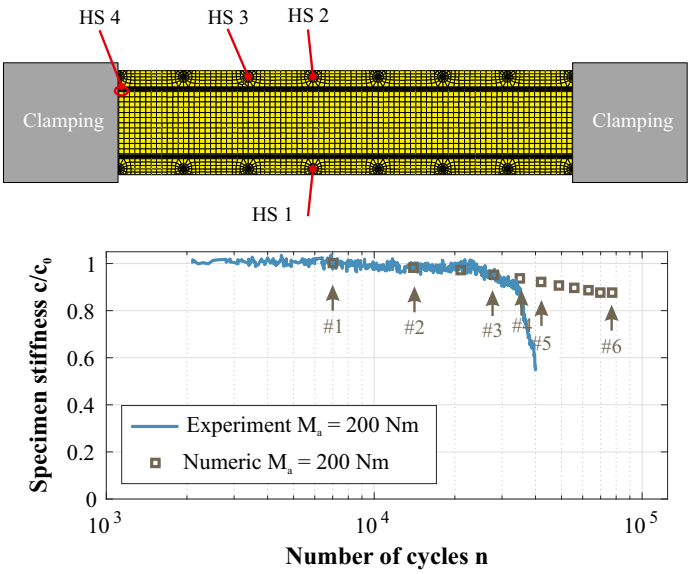

Fig. 12. Stiffness results RP hat specimen $R = 0.1$, $M_a = 200\,\text{Nm}$

		HS1	HS2	HS3	HS4
# 1	D_{it}	**0.15**	0.15	0.13	0.07
	$\sigma_{vm}/\sigma_{HS\,1max}$	**1**	1	0.97	-
	d_{spot} in mm	**3.5**	3.5	3.7	-
# 2	D_{it}	0.12	**0.13**	0.2	0.09
	$\sigma_{vm}/\sigma_{HS\,1max}$	0.94	**0.97**	0.95	-
	d_{spot} in mm	2.9	**2.8**	2.9	-
# 3	D_{it}	0.08	0.07	**0.10**	0.09
	$\sigma_{vm}/\sigma_{HS\,1max}$	0.92	0.89	**0.95**	-
	d_{spot} in mm	2.5	2.5	**2.4**	-
# 4	D_{it}	0.07	**0.11**	0.07	0.09
	$\sigma_{vm}/\sigma_{HS\,1max}$	0.89	**0.93**	0.89	-
	d_{spot} in mm	2.3	**2.0**	2.3	-
# 5	D_{it}	0.07	0.06	0.07	**0.10**
	$\sigma_{vm}/\sigma_{HS\,1max}$	0.89	0.86	0.90	**-**
	d_{spot} in mm	2.1	1.6	2.1	**-**
# 6	D_{total}	0.87	0.92	0.86	**1.04**

Table 4. Damage (D), normalized equivalent stress signed von Mises($\sigma_{vm}/\sigma_{HS\,1max}$) and spot diameter ($d_b$) at selected hot-spots

are promising. The methodology could be implemented using available software and output formats. Basic failure mechanisms can be represented and the numeric stiffness behaviour until the specimens final failure can be simulated. The actual stiffness decrease at the rupture of the whole specimen cannot be simulated, which might be due to the chosen degradation law and / or its parametrization or the linear FE modelling and will be focus of further research.

5. Summary and Outlook

Several numerical and experimental analyses and a first numerical approach with regards to the fatigue and degradation behaviour of various joining techniques were presented in this paper. The joining processes and different fatigue assessment approaches (focusing on the fatigue assessment of spot welds) are introduced. Experimental results are shown for various specimen geometries. For each joining technique a micrographic analysis is performed and used for the FE modelling. General fatigue life results and the corresponding damage mechanisms are shown for the analysed joints and specimens. The arc welded hat profile failed due to different damage mechanisms which results in an increased scatter. In addition the stiffness behaviour of each joint and specimen is shown. Two main assumptions -

the independence of the degradation behaviour and load direction / material combinations - for the later introduced methodology are derived and first indications of permissibility are presented.
In addition to the experimental results a methodology to assess stiffness degradation in fatigue simulation and its feasibility is shown. It considers changes in stiffness based on the accumulated damage in the joint in an iterative computation process. The methodology has been derived for spot welded specimens. As an computation example the spot welded hat specimen was selected. To implement the methodology material and computation parameters are necessary. The stiffness behaviour of spot welded peal and shear specimens is used to determine the material parameters for the degradation simulation. The degradation behaviour of local stress-states within peal and shear stress are interpolated. The used degradation law is a simple power law solely to prove the feasibility of the methodology. The derived material parameters are used to simulate the stiffness behaviour of the spot welded hat specimen. The first results look promising as the initial stiffness decrease can be represented accurately. The final failure of the specimen cannot be predicted at the moment. A reason might be the degradation law and corresponding parameters.

Several aspects of the paper should be scope of future work. At first the main assumptions need to be investigated in detail as the current verification is based on only a small dataset. In the automotive industry often multiple joining techniques are used on one component, which leads to the necessity to test the methodology on hybrid specimens. On the numerical side the degradation law and the criteria for the interpolation of the stiffness behaviour between different stress states needs to be adapted.

[1] Boellhoff Gruppe, RIVTAC® Automation P: Bolzensetzen in Hochgeschwindigkeit Innovativ und flexibel, 2016.
[2] Verband der Automobilindustrie, xMCF: A Standard for Describing Connections and Joints in the Automotive Industry: FAT289, 2016.
[3] A. H. Fritz, G. Schulze (Eds.), Fertigungstechnik, VDI-Buch, Springer-Verlag Berlin Heidelberg, Berlin, Heidelberg, 8., neu bearbeitete auflage edn., ISBN 978-3-540-76695-7, doi:10.1007/978-3-540-76696-4, 2008.
[4] J. D. Majumdar (Ed.), Laser-assisted fabrication of materials, vol. 161 of *Springer series in materials science*, Springer, Heidelberg u.a., ISBN 978-3-642-28359-8, 2013.
[5] H. Hanselka, K. Störzel, T. Bruder, Überlasten und ihre Auswirkungen auf die Betriebsfestigkeit widerstandspunktgeschweißter Feinblechstrukturen: FAT239, Berlin, 2012.
[6] Y. Nakahara, M. Takahashi, A. Kawamoto, M. Fujimoto, N. Tomioka, Method of Fatigue Life Estimation for Spot-Welded Structures, in: SAE 2000 World Congress, SAE Technical Paper Series, SAE International400 Commonwealth Drive, Warrendale, PA, United States, 2000.
[7] FEMFAT 5.2 - Spot User Manual, 2015.
[8] P. Rösch, T. Bruder, P. Wagner, Fatigue and degradation behaviour of carbon fibre reinforced plastics, in: M. Vormwald, T. Beier, K. Breidenbach (Eds.), Proceedings of the 5th Symposium on Structural Durability in Darmstadt, vol. 5, Darmstadt, ISBN 978-3-939195-55-9, 43–56, 2017.
[9] J. Degrieck, W. van Paepegem, Fatigue damage modeling of fibre-reinforced composite materials: Review, Applied Mechanics Reviews 54 (4) (2001) 279, ISSN 00036900.
[10] H. T. Hahn, R. Y. Kim, Fatigue Behavior of Composite Laminate, Journal of Composite Materials 10 (2) (1976) 156–180, ISSN 0021-9983.
[11] T. Seeger, S. Greuling, J. Brüning, P. Leis, C. M. Sonsino, D. Radaj, Bewertung lokaler Berechnungskonzepte zur Ermüdungsfestigkeit von Punktschweißverbindungen, 2005.
[12] J. Draisma, J. L. Overbeeke, Fatigue characteristics of heavy-duty spot-welded lap joints, Metal construction and British welding journal (7) (1974) 213–219.
[13] D. Radaj, C. M. Sonsino, W. Fricke, Fatigue assessment of welded joints by local approaches, Woodhead publishing in materials, Woodhead, Cambridge, 2. ed. edn., ISBN 978-1-85573-948-2, 2006.
[14] T. Satoh, H. Abe, K. Nishikawa, M. Morita, On three-dimensional elastic-plastic stress analysis of spot-welded joint under tensile shear load, Transactions of the Japan welding society 22 (1) (1991) 46–51.
[15] Yuuki Ryoji, T. Ohira, H. Nakatsukasa, W. Yi, Fracture mechanics analysis and evaluation of the fatigue strength of spot welded joints, Transactions of the Japan Society of Mechanical Engineers Series A 51 (467) (1985) 1772–1779, ISSN 0387-5008, doi:10.1299/kikaia.51.1772.
[16] O. Hahn, R. Kurzok, A. Rohde, Untersuchungen zur Übertragbarkeit von Kennwerten einer punktgeschweißten Einelementprobe auf Mehrelementprüfkörper und Bauteile: FAT142, Berlin, 1998.
[17] D. Gieske, Beitrag zur Prüfung punktförmiger Blechverbindungen, Ph.D. thesis, 01.01.1995.
[18] DVS – Deutscher Verband für Schweissen und verwandte Verfahren, Prüfen von Widerstandspressschweißverbindungen, 2009.
[19] Siemens Industry Software GmbH, LMS Virtual.Lab Durability Solver Training: Software Traning, 2016.